DEUTSCHES ELEKTRONEN-SYNCHROTRON DESY

DESY SR 84-25
December 1984

Eigentum der DESY Bibliothek
Property of DESY library
Zugang: 11. FEB. 1985
Accessions:
Leihfrist: 7 Tage
Loan period: 7 days

X-RAY STANDING WAVE ANALYSIS OF BISMUTH IMPLANTED IN Si(110)

by

N. Hertel

Institute of Physics, University of Aarhus, Aarhus, Denmark

G. Materlik

Hamburger Synchrotronstrahlungslabor HASYLAB at DESY

J. Zegenhagen

II. Institut f. Experimentalphysik, Universität Hamburg

ISSN 0723-7979

NOTKESTRASSE 85 · 2 HAMBURG 52

DESY behält sich alle Rechte für den Fall der Schutzrechtserteilung und für die wirtschaftliche Verwertung der in diesem Bericht enthaltenen Informationen vor.

DESY reserves all rights for commercial use of information included in this report, especially in case of filing application for or grant of patents.

To be sure that your preprints are promptly included in the
HIGH ENERGY PHYSICS INDEX ,
send them to the following address (if possible by air mail) :

DESY
Bibliothek
Notkestrasse 85
2 Hamburg 52
Germany

DESY SR 84-25
December 1984

ISSN 0723-7979

X-Ray Standing Wave Analysis of Bismuth Implanted in Si(110)

N. Hertel[(1)], G. Materlik[(2)] and J. Zegenhagen[(3)]*

(1) Institute of Physics, University of Aarhus, DK-8000 Aarhus C, Denmark

(2) Hamburger Synchrotronstrahlungslabor HASYLAB at DESY, Notkestr. 85, D-2000 Hamburg 52, Germany

(3) II. Institut für Experimentalphysik, Universität Hamburg, Luruper Chaussee 149, D-2000 Hamburg 50, Germany

* present address: Physics Department, SUNYA, 1400 Washington Avenue, Albany, N.Y. 12 222, USA

Abstract

Perfect crystal silicon samples implanted with 60 KeV Bi atoms along the [110] surface normal direction were analyzed with X-ray standing waves. Two reflection orders, (220) and (440) were used with synchrotron radiation to study systematically the impurity distribution function at 5 different doses ranging from 0.6 to 10 x 10^{14} Bi atoms/cm^2. The analysis reveals the substitutional Bi position connected with a lattice expansion and the formation of precipitates at higher Bi doses as well as estimates for the Bi vibrational amplitude.

to be published in : Z. Phys. B - Condensed Matter 58, (1985)

As demonstrated by Golovchenko et al. /1/, structural information about impurities in perfect crystals can be obtained by measuring the fluorescence yield from foreign atoms while scanning in angle through a strong Bragg diffraction condition of the host lattice. In such a scan, the standing X-ray wavefield, which is generated by the interference of the incident and reflected beams and which has the spatial periodicity of the (h,k,l) diffraction planes, moves continuously by one-half of a diffraction plane spacing in the -H direction. Correspondingly, the variation of the fluorescence yield from impurity atoms depends on the position of such atoms relative to the chosen diffraction planes. The basic assumption commonly made to analyze the fluorescence yield spectra /1,2/ is that the implanted atoms either occupy single distinct lattice sites or that they are distributed incoherently within the substrate lattice.

However, a more detailed analysis of the distribution function of implanted impurity atoms has to include aspects such as: impurity-vacancy interaction, formation of impurity precipitates, lattice relaxation, and lattice distortion around the impurity sites /3/. In this context it is important to realize that the X-ray standing wave analysis using the m-th reflection order from a fundamental set of diffraction planes (h,k,l) will determine the m-th Fourier component of the impurity distribution function in the direction of H. In the present paper we have therefore applied a (220) X-ray standing wave analysis with first and second reflection order to the Si(Bi) system at different Bi doses well above the solubility limit. The results are compared with a realistic model of the Bi distribution function to reach more quantitative information about the Bi distribution.

Several groups have performed comprehensive studies of the Si(Bi) system /4-8/, mostly using the Rutherford backscattering-channeling technique. Most of these studies /4-7/ conclude that part of the Bismuth occupy substitutional

sites while part are displaced slightly from lattice positions. However, later studies have demonstrated the existence of a beam effect for As /9-11/, Sb /4/ and Bi /11/ in Si causing the impurity atoms to be displaced from substitutional positions under the influence of the analyzing beam. This effect has been shown to be dose dependent, and one group /8/ used this information to perform a planar channeling study of Bi in Si in which the effect of the analyzing beam was eliminated. This measurement concluded that Bi in Si is substitutional, but with a narrow distribution around Si positions because of lattice strain in the neighbourhood of the Bi atoms.

All of these above mentioned measurements have been performed using dopant concentrations exceeding the solid solubility limit (8×10^{17} cm^{-3} for Bi in Si /12/) as is the case in the present work. Recent channeling measurement coupled with careful thermal treatment of supersaturated Bi implants have shown evidence /13/ that the dopant precipitates out as partially coherent crystallites upon annealing to a temperature which is dose dependent. These results are also in agreement with studies of the Si(Sb) system which shows similar effects /14/ being most likely due to concentration enhanced diffusion /15/ mediated by defects or vacancies.

As we will show, the result of our present study with X-ray standing waves are consistent with such a model in which part of the Bi atoms form precipitates possibly assuming a Bi hexagonal structure if they are large enough, but at least aligned to the Si structure along the edges. Since this technique measures the phase of the distribution function relative to the deep lying, perfect Si planes, this model corresponds to one in which part of the dopant atoms are distributed symmetrically around lattice sites and part are arranged incoherently with respect to the host lattice.

For the measurement of the present set of data on the Si(Bi) system with reflection orders (220) and (440), we use a photon polarization direction perpendicular to the reflection plane and an implantation depth and connected straggling range of the implanted Bi each being small /16/ compared to the extinction depth of the incident X-rays.

The dynamical theory of x-ray diffraction /17/ predicts that one Bloch-wave eigenstate of the photon is excited inside the crystal under the condition of Bragg diffraction. For a two-beam Bragg-case and an incident plane wave $\underline{E}_o$ $\exp(-i(2\pi \underline{K}_o^i \cdot \underline{r} - \omega t)$, this photon wavefield consists of two partial plane waves. Their amplitudes are summed up to calculate the intensity I of the total $\underline{D}$ field at the position $\underline{r}$ as

$$I(\vartheta,r) = |D_o \exp(-i(2\pi \underline{K}_o \cdot \underline{r} - \omega t)) + \underline{D}_H \exp(-i(2\pi(\underline{K}_o + \underline{H}) \cdot \underline{r} - \omega t))|^2 \quad . \tag{1}$$

Setting $R = |\underline{D}_H|^2 / |\underline{D}_o|^2$, $D_H(\vartheta) = D_o(R)^{1/2} \exp(iv(\vartheta))$ and $\mu_z(\vartheta) = 4\pi \, \mathrm{Im}(K_o)$, where the z-axis is directed inward perpendicular to the crystal surface, which is assumed to be parallel to the diffraction planes, gives

$$I(\vartheta,\underline{r}) = \exp(-\mu_z(\vartheta)z)(1+R(\vartheta)+2(R(\vartheta))^{1/2}\cos(v(\vartheta)-2\pi\underline{H}\cdot\underline{r})) \quad . \tag{2}$$

R and v describe the intensity and the phase of the reflected wave relative to the incident wave as a function of reflection angle ϑ.

The probability for emission of a fluorescence photon from an atom at position $\underline{r}$ is proportional to the wavefield intensity $I(\vartheta, r)$ provided the photon energy is sufficient to excite a photoelectron in this atom. When a specific atomic species is described by a normalized density function $\rho(\underline{r})$ the fluorescence yield will be proportional to $\int \rho(\underline{r}) \, I(\vartheta,\underline{r}) d^3r$ where the integral

has to be evaluated over the volume V which contributes to the photon yield. Throughout this paper we shall assume that $\rho(\underline{r})$ is only different from zero over a crystal depth region which is close to the surface and small compared to the extinction depth which is defined as the minimum of μ_z^{-1} when the diffraction condition is passed.

Normalization of the yield at an angle ϑ within the range of a Bragg reflection to that at a reflection angle with zero reflectivity, eliminates the dependence on geometrical parameters, on cross sections, and on detection efficiency. We therefore define a normalized angular dependent fluorescence yield Y_H which is obtained from a standing wave measurement with a spatial periodicity $d_H = 1/|\underline{H}|$ for a cubic structure, as

$$Y_H(\vartheta,\underline{r}) = 1+R_H(\vartheta)+2(R_H(\vartheta))^{1/2}N^{-1}\int_V \rho(\underline{r})\cos(v_H(\vartheta)-2\pi\underline{H}\cdot\underline{r})d^3r \tag{3}$$

N gives the total number of fluorescence selected atoms with $\int_V \rho(\underline{r})d^3r = N$, being implanted impurity atoms in our present study. $\underline{H}\cdot\underline{r}$ gives the position in units of the diffraction plane spacing and it is convenient to introduce a coordinate z_H (in the direction of z) perpendicular to the plane by $z_H = (n+z_R)d_H$, where the integer n runs from zero to infinity and $z_R = \Delta d/d_H$. The integration of $\rho(\underline{r})$ in a plane parallel to the diffraction planes defines a z_H-dependent distribution function $P(z_H)$ with $\int_{z_H} P(z_H)dz_H = 1$. We further introduce the reflection order m of the first non forbidden reflection $\underline{H}$ in (1) and get

$$Y_m(\vartheta,z_H) = 1+R_m(\vartheta)+2(R_m(\vartheta))^{1/2}\int_{z_H} P(z_H)\cos(v_m(\vartheta)+2\pi\, mz_H/d_H)dz_H \tag{4}$$

For simplicity we have omitted the index H from all quantities which are already characterized by subscript m. Replacing the cosine in (4) by the sum of two exponentials shows that the interference term is proportional to the

m-th Fourier component

$$F_m(P) = \int_0^1 P(z_R)\exp(2\pi imz_R)dz_R = f_{c,m}\exp(2\pi i\Phi_{c,m}) \tag{5}$$

of the z_H-projected density $P(z_H)$. We can thus write

$$Y_m(\vartheta,z_H) = 1+R_m(\vartheta)+2(R_m(\vartheta))^{1/2}f_{c,m}\cos(v_m(\vartheta)+2\pi\Phi_{c,m}) \tag{6}$$

In our standing wave analysis the measured yield data $Y_m^H(\vartheta)$ are given a least-square fit to (6). $R_m(\vartheta)$ is simultaneously measured with $Y_m(\vartheta)$ and $v_m(\vartheta)$ is calculated from dynamical theory /17/. The result is expressed by $f_{c,m}$ and $\Phi_{c,m}$ which are called the coherent fraction and coherent position, respectively, and which are the amplitude and phase of the m-th Fourier component of the z_H-projected density function of fluorescence selected atoms.

A realistic model for $P(z_R)$ in the case of implanted Bi atoms in Si(110) has to express broadening by thermal vibrations, possible lattice distortion in the vicinity of the Bi atoms as well as concentration dependent lattice relaxation which will change the lattice constant in the implanted region relative to that of the bulk planes. These later planes determine the periodicity of the standing wave pattern. Furthermore, a fraction A_u of the Bi can remain randomly distributed with respect to the wave field periodicity. This is for example the case when the surface of the sample is covered by some disordered oxide layers which can also trap some Bi. To simplify the analysis we shall assume that $(1-A_u)$ atoms are occupying one lattice site only on the scale of z_R.

The following convoluted distribution function includes these different aspects:

$$P(z_R) = A_S P_T(\sigma_T, z_R) \otimes P_D(\sigma_D, z_R) \otimes P_r(z_{r,o}, z_R) + A_u \quad , \qquad (7)$$

where $A_u + A_s = 1$. Thermal vibrations are represented by a normalized Gaussian distribution with

$$P_T(\sigma_T, z_R) = ((2\pi)^{1/2}\sigma_T)^{-1} \exp(-z_R^2/2\sigma_T^2) \qquad (8)$$

with

$$\sigma_T = (\langle u_H^2 \rangle)^{1/2}/d_H \qquad (9)$$

where $(\langle u_H^2 \rangle)^{1/2}$ is the Bi root mean square vibrational amplitude in the $\underline{H}$ direction. The distortion profile P_D can also be approximated by a Gaussian with a standard deviation σ_D, and the function $P_r(z_{r,o}, z_R)$ which describes the effect of lattice relaxation on $P(z_R)$ is determined by the concentration profile of the implanted atoms which is also Gaussian like in z_H-direction /16/. A concentration proportional lattice relaxation causes a shift of the doped lattice planes relative to the underlying undisturbed crystal diffraction planes. A quadratic expression

$$P_r(z_{r,o}, z_R) = 3/4 \, (z_{r,o})^{-3} \, (z_{r,o}^2 - z_R^2) \qquad (10)$$

is a reasonable approximation for the resulting relaxation profile. The coordinate $z_{r,o}$ describes the mean integrated lattice expansion.

By using the convolution theorem of Fourier transformations we write $f_{c,m}$ of (6) as a product of the amplitudes of the m-th Fourier components of P_T, P_D, and P_r:

$$f_{c,m} = f_{T,m} \, f_{D,m} \, f_{r,m} \quad . \qquad (11)$$

These corresponding amplitudes can be evaluated as follows:

$$f_{T,m} = D_H = \exp(-2\pi^2 m^2 \sigma_T^2) \qquad (12)$$

which is well known as the Debye-Waller factor. The product with $f_{D,m}$ can be written as

$$f_{G,m} = f_{T,m} \, f_{D,m} = \exp(-2\pi^2 m^2 (\sigma_T^2 + \sigma_D^2)) \quad . \qquad (13)$$

For the Fourier amplitude of P_r we obtain

$$f_{r,m} = 3(2\pi m z_{r,o})^{-3} (\sin(2\pi m z_{r,o}) - (2\pi m z_{r,o}) \cos(2\pi m z_{r,o})) \quad . \qquad (14)$$

Only the Fourier component of P_r has a phase $\Phi_{r,m}$ different from zero since the Gaussian used for P_T and P_D is a real and even function. Therefore $\Phi_{c,m} = m \cdot z_{r,o}$.

Although the distribution function (7) contains several independent parameters we shall show that multiple order x-ray standing wave measurements coupled with systematic dose dependent measurements can be used to characterize the distribution function.

The experiments were carried out at the ROEMO instrument of the Hamburg Synchrotron Radiation Laboratory HASYLAB using the storage ring DORIS as a radiation source. The white incident synchrotron X-radiation beam (SXR) was monochromatized by a slightly dispersive double crystal monochromator (see Fig. 1). The first crystal X1 was a symmetric Ge(220) crystal reflecting in

first or second order and the plane wave generating second crystal X2 was Silicon(220) with an asymmetry factor $(b)^{1/2} \approx 3.6$ or Silicon(440) with an asymmetry factor $(b)^{1/2} \approx 2.3$ for the (220) and (440) measurement, respectively. b is defined as the ratio $\sin(\vartheta_B+\varphi)/\sin(\vartheta_B-\varphi)$, where ϑ_B is the Bragg angle and φ the angle between the diffraction planes and the surface.

The monochromatic photon beam with an energy of E_γ = 15.4 keV and 15.2 keV and a vertical angular collimation of 3.6 µrad and 2.2 µrad for the (220) and (440) case, respectively, was impinging on the implanted Si sample crystal XS illuminating an area of 14 mm^2 and 140 mm^2 respectively. The area was chosen by collimators S2 and S3. The sample was placed on a goniometer which was continuously rocked back and forth in angle ϑ through the rocking curve with a sweep frequency of 0.1 Hz, while a Si(Li) solid state detector (SSD) simultaneously collected approximately 0.3 srad from the scattered spectrum, emitted by the implanted crystal. A NaI detector and an ion chamber I_2 were used to measure the crystal reflectivity. These data from I_1, I_2, SSD, and NaI were stored into a multi-channel analyzer operating in a multi-spectrum-scaling mode. The SSD was aligned such that it detected the horizontally scattered photons perpendicular to the vertical reflection plane to reduce the Compton and TDS spectral contribution, since SXR is linearly polarized with the $\underline{E}$ vector pointing horizontally. This instrument is described in detail in /18/, /19/ and /20/.

The samples were implanted at room temperature and 60 keV energy with Bi atom doses ranging from 6×10^{13} to 1.0×10^{15} Bi atoms/cm^2. Subsequently, they were annealed in four stages in a dry N_2 atmosphere. First they were brought in 30 minutes to 775°C, a temperature which was then held for 30 minutes. The cooling process was gradually carried out in 60 minutes down to 500°C and finally down to 50°C in 120 minutes.

The rocking curves and fluorescence yield data shown in Fig. 2 were measured at a DORIS energy of 5.0 GeV and a medium electron current of 25 mA. A signal from a random pulse generator was used to correct each spectral region for deadtime effects which were caused by the strongly varying count rate. The background in the spectral region of the Bi L lines was determined for such run by a reference measurement for which the non-implanted backside of each sample was used. Pb and Pt lines, although being present with a low signal, had to be taken into account especially for the lower Bi dose measurements. Because of these neighbouring lines the background below the Bi lines was approximated by a quadratic polynomial and subtracted from the total peak area to determine the Bi yield instead of using a Gaussian peak fit procedure. Accordingly the data shown in Fig. 2 were normalized to the pulser signal and to the primary monochromatic SXR intensity, corrected for spurious fluorescence lines and were normalized to the fluorescence yield obtained for zero reflectivity. A χ^2-fit of (6) to these data is also shown in Fig. 2 and the parameters $\Phi_{c,H}$ and $f_{c,H}$ are listed in Table 1 for H = (220) and (440). The angular scale was determined by a χ^2-fit of the reflectivity curve to the theoretical expression inferred from the dynamical theory of X-ray diffraction and convoluted with the monochromator angular emittance. As can readily be seen $f_{c,220}$ and $f_{c,440}$ deviate from each other for all Bi doses and increase with decreasing impurity content. All measured phases $\Phi_{c,H}$ deviate from zero but as expected this is most pronounced for higher impurity concentrations since the integrated lattice expansion increases accordingly. A mean integrated lattice expansion <Δd> was determined from a weighted average of $\Phi_{c,220}$ and $\Phi_{c,440}$ and is also listed in Table 1. These measured values of the lattice relaxation were used to deduce parameters $f^r_{c,H}$ according to (11) and (13) by the relation $f^r_{c,H} = f_{c,H}\, f^{-1}_{G,H}$. However, this procedure hardly changes the amplitudes.

From (11) and (12) we may determine the standard deviation of the Gaussian distribution caused by thermal vibrations and distortion as

$$\sigma^2 = \sigma_T^2 + \sigma_D^2 = 1/(6\pi^2)\ \ln\,(f^r_{c,220}/f^r_{c,440}) \quad . \tag{15}$$

The results listed in Table 1 do not show a pronounced dose dependence. Even the highest dose value only deviates slightly from the dose mean value $\langle\sigma^2\rangle$ which was used to calculate substitutional fractions $A_{s,220}$ and $A_{s,440}$ and the weighted average A_s, also listed in Table 1, by using the relation $A_{s,H} = f^r_{c,H}\, D_H^{-1}(\langle\sigma_H^2\rangle)$. To demonstrate the close connection between lattice relaxation and the total number of Bi atoms on substitutional sites, a parameter $r_s = \langle\Delta d\rangle / A_s /$ Bi-dose is also included in Table 1 and remains constant for all measured Bi concentrations.

This point is further illustrated in Fig. 3. The linear dependence in a semi-logarithmic plot of the substitutional Bi amount and lattice relaxation on the total amount of implanted Bi atoms is remarkable.

As shown in Fig. 4 the results of the present X-ray standing wave analysis can be directly compared with Rutherford backscattering studies from Campisano et al. /13/. The dependence of the substitutional Bi fraction A_s on the total Bi dose is very similar for both studies. The visible deviations for higher Bi concentrations can be caused by a difference in the applied annealing processes, since the precipitation is diffusion controlled and therefore depending on the annealing temperature, time and cycle structure.

From these results it can be concluded that a supersaturated solid solution of Bi in Si is formed up to a dose of about 10^{14} Bi atoms/cm^2 (Fig. 4), with an exclusively (within the present error bars) substitutional Bi site. The

increase of the randomly distributed Bi fraction in connection with the linear increase of the total substitutional Bi amount and of the integrated lattice relaxation with increasing total impurity dose finds a proper explanation in the formation of precipitates. Since their formation does not effect the silicon lattice relaxation in a distinguishable way, one can conclude that they align well with the silicon lattice. The lattice relaxation which is caused by the substitutional fraction can be calculated to be (0.08 ± 0.01)Å/10^{14} substitutional Bi atoms/cm^2.

There is no significant indication from our data that anything else but thermal vibrations cause the Gaussian-like distribution profile characterized by $\langle\sigma^2\rangle$ which leads to the differences between $f^r_{c,220}$ and $f^r_{c,440}$. We may thus calculate the Bi root mean square vibrational amplitude at 300 K to be $(\langle u^2_{220}\rangle)^{1/2} = (0.16 \pm 0.04)$Å which is a reasonable result in comparison to the corresponding bulk values of Si (0.08 Å), when the larger Bi mass is taken into account, and Bi (0.11 Å).

This picture is consistent with our measurement up to concentrations of 7 x 10^{14}/cm^2. The highest dose result at 10^{15}/cm^2, however, possibly indicates that a further modification of the distribution function is needed at higher doses. The σ^2 value is high in comparison to the lower dose values and the Δd_{220} and Δd_{440} result inferred from $\Phi_{c,220}$ and $\Phi_{c,440}$ show a remarkable deviation from each other Only more systematic measurements at such high doses can clarify this aspect.

The financial support by the Bundesministerium für Forschung und Technologie for part of the project is gratefully acknowledged.

References

1 Golovchenko, J.A., Batterman, B.W. and Brown, W.L. Phys. Rev. B10, 4239 (1974)

2 Andersen, S.K., Golovchenko, J.A. and Mair, G., Phys. Rev. Lett. 37, 1141 (1976)

3 see e.g.: "Point Defects in Semiconductors" by Lannoo, M. and Bourgoin, J. in: Springer Series in Solid-State Sciences, Vol. 22 and 23 (Springer Verlag)

4 Eriksson, L., Davies, J.A., Johansson, N.G.E. and Mayer, J.W., J. Appl. Phys. 40, 842 (1969)

5 Sigurd, D. and Domeij, B., Phys. Lett. 36A, 81 (1971)

6 Picraux, S.T., Brown, W.L. and Gibson, W.M., Phys. Rev. B6, 1382 (1972)

7 Sigurd, D. and Björquist, K., Rad. Effects 17, 209 (1973)

8 Wagh, A.G., Radhakrishnan, S., Gaonkar , S.G. and Kansara, M.S., Nucl. Instr. and Meth. 168, 191 (1980)

9 Haskell, J., Rimini E., and Mayer, J.W., J. Appl. Phys. 43, 3425 (1972)

10 Kool, W.H., Roosendaal, H.E., Wiggers L.W. and Saris, W.F., Nucl. Instr. and Meth. 132, 285 (1976)

11 Wiggers, L.W. and Saris, F.W., Nucl. Instr. and Meth. 149, 399 (1978)

12 Trumbore, F., Bell Syst. Tech. J. 39, 575 (1960)

13 Campisano, S.U., Rimini, E., Baeri, P., Foti, G.: Appl. Phys. Lett. 37, 170 (1980)

14 Pogany, A.P., Preuss, T., Short, K.T., Wagenfeld H.K., Williams, J.S.: Nucl. Instr. and Meth. 209/210, 731 (1983)

15 Frank, W., Seeger, A., Gösele, U.: In: Defects in Semiconductors, eds. Narayan, J., Tan, T.Y. (North Holland, Amsterdam, 1981) p. 31

16 O'Connor, D.J., Nucl. Instr. and Meth. 196, 493 (1982)

17 Laue, M.v., Röntgenstrahlinterferenzen, 3rd ed., Frankfurt, Akademische Verlagsgesellschaft (1960)

18 Krolzig, A., Materlik, G., Zegenhagen, J., Nucl. Instr. and Meth. 208, 613 (1983)

19 Krolzig, A., Materlik, G., Swars M., and Zegenhagen, J., Nucl. Instr. and Meth. 219, 430 (1984)

20 Materlik G., and Zegenhagen, J., Phys. Lett. 104A, 47 (1984)

Table 1

DOSE (10^{14} cm^{-2})	$\phi_{c,220}$	$\phi_{c,440}$	$\langle \Delta d \rangle$ (Å)	$f_{c,220}$	$f_{c,440}$	$f^{r}_{c,220}$	$f^{r}_{c,440}$	c^2 $\times 10^3$	$A_{s,220}$	$A_{s,440}$	A_s	r_s (Å)
0.6	0.025 ±0.02		0.05 ±0.035	0.79 ±0.08		0.79			0.90		0.90 ±0.08	0.1 ±0.07
1.0	0.031 ±0.014	-0.003 ±0.05	0.035 ±0.03	0.84 ±0.07	0.66 ±0.15	0.84	0.66	4.1 ±4.1	0.96	1.13	1.01 ±0.08	0.04 ±0.04
4.0	0.055 ±0.008	0.09 ±0.025	0.10 ±0.01	0.61 ±0.02	0.44 ±0.07	0.62	0.46	6.6 ±3.5	0.71	0.79	0.73 ±0.03	0.035 ±0.004
7.0	0.076 ±0.01	0.13 ±0.024	0.135 ±0.01	0.38 ±0.02	0.28 ±0.05	0.39	0.30	4.4 ±3.0	0.45	0.51	0.47 ±0.03	0.040 ±0.004
10.0	0.085 ±0.009	0.10 ±0.022	0.135 ±0.035	0.36 ±0.02	0.18 ±0.02	0.37	0.19	11.3 ±3.0	0.42	0.32	0.37 ±0.05	0.04 ±0.01

$\langle \sigma^2 \rangle = (6.8 \pm 1.7) \times 10^{-3}$

$r_s = \frac{\langle \Delta d \rangle}{A_s \, \mathrm{DOSE}}$ = lattice relaxation per 10^{14} substitutional Bi atoms per cm^2

$\langle r_s \rangle = (0.04 \pm 0.005)$Å$/(10^{14}$ Bi-atoms$/cm^2)$

Figure Captions

Figure 1 Experimental arrangement (schematic). For detailed description see text.

Figure 2 Measured and calculated reflectivity and Bi fluorescence yield curves for (a) Si(220) and (b) Si(440) reflections. The yield curves of crystals with different Bi implantation doses were shifted for doses smaller $10^{15}/cm^2$ on the fluorescence yield scale.

Figure 3 Measured mean integrated Si lattice expansion and the measured amount of substitutional Bi atoms as a function of total implanted Bi dose.

Figure 4 Measured substitutional fraction of Bi atoms as function of total implanted Bi dose.

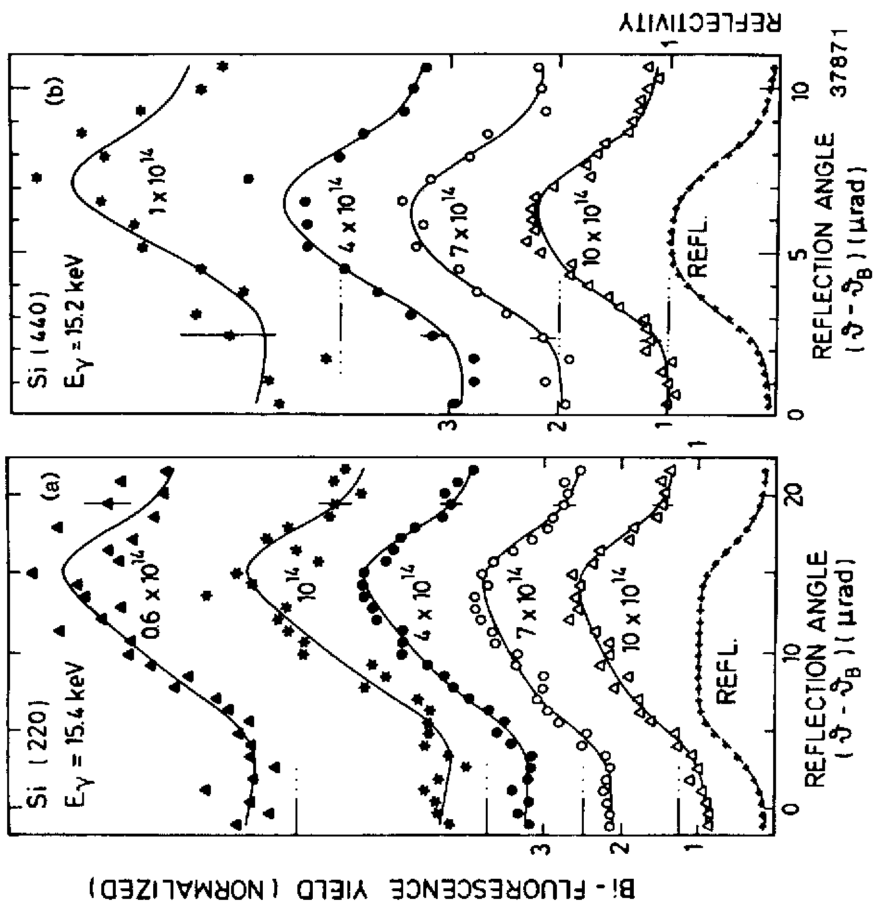

Fig. 2

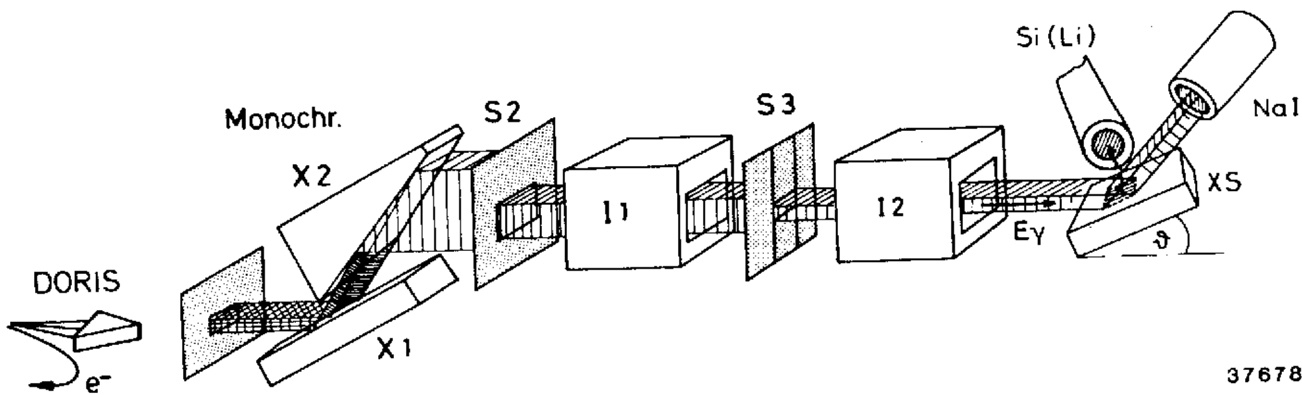

Fig. 1

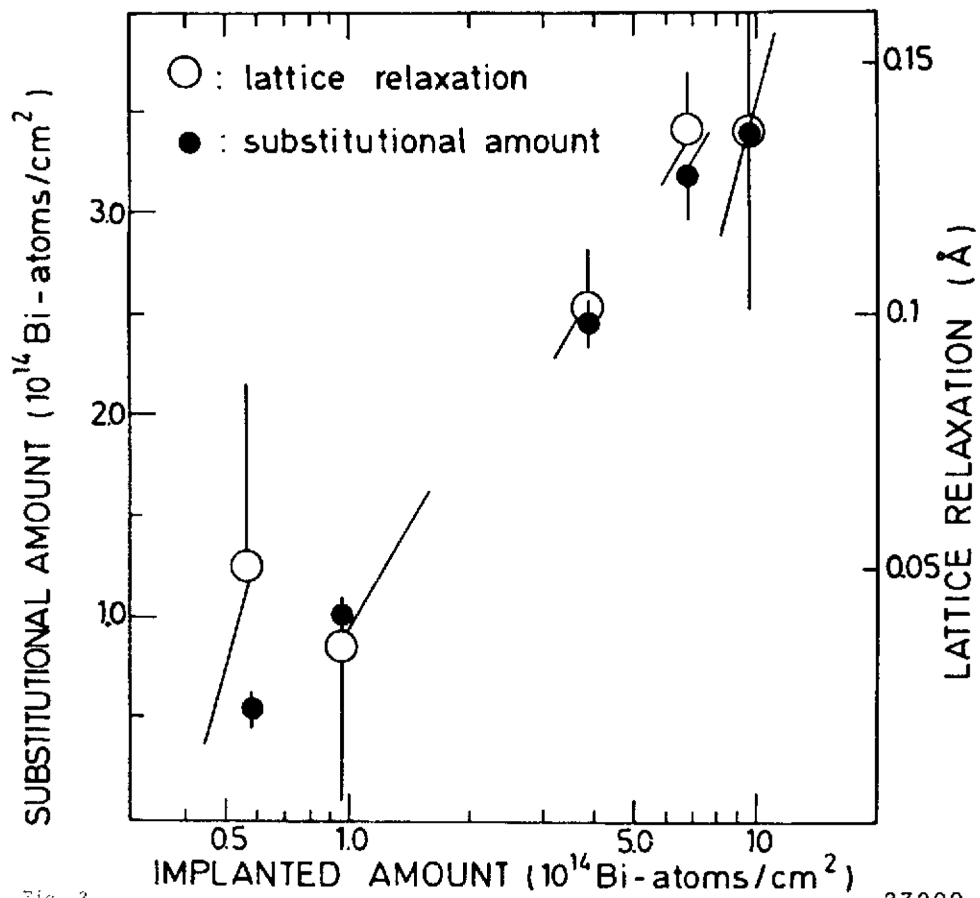

Fig. 3

37209

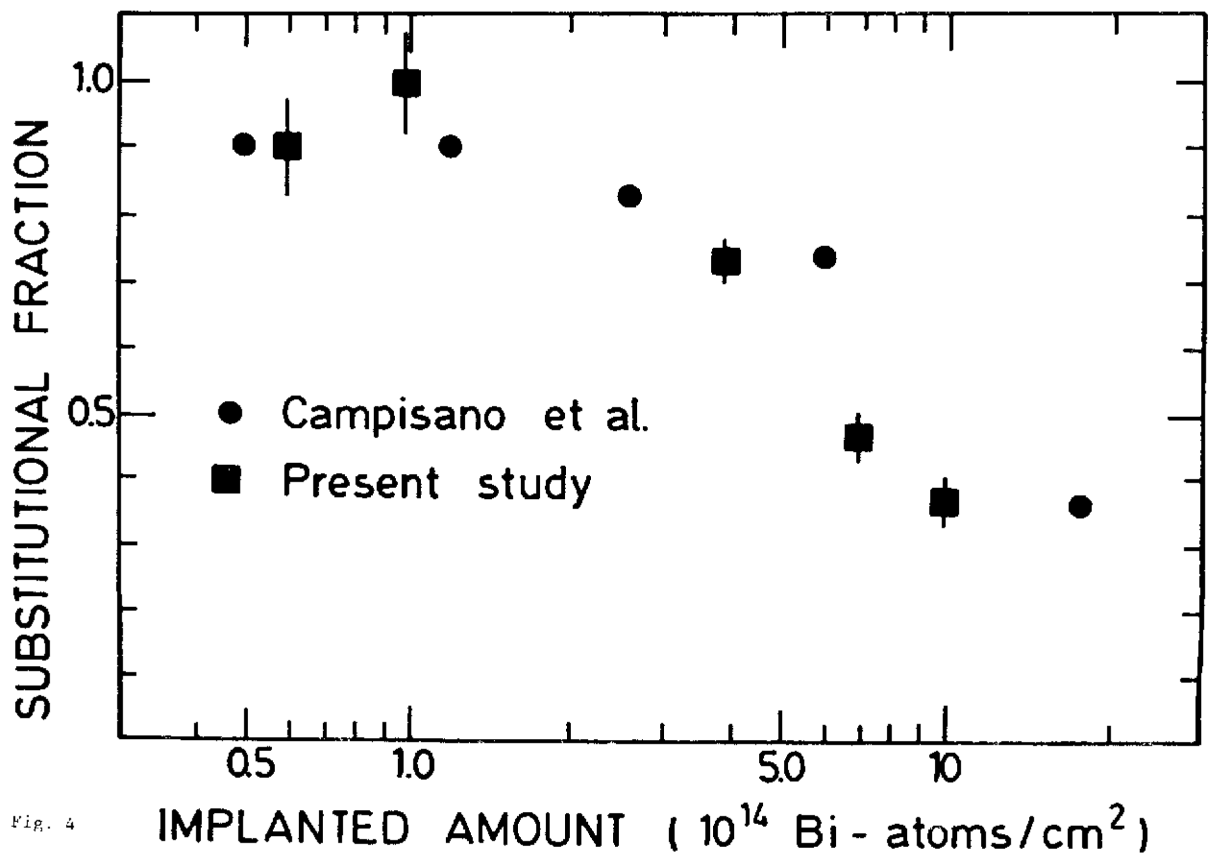

Fig. 4

37210